J|A|C|S
ARTICLES
Published on Web 01/23/2003

Synthesis, Structure, and Magnetic Properties of the Fullerene-Based Ferromagnets Eu_3C_{70} and Eu_9C_{70}

Taishi Takenobu,[†,‡] Dam H. Chi,[§] Serena Margadonna,[∥] Kosmas Prassides,*[,⊥] Yoshihiro Kubozono,[‡,○] Andrew N. Fitch,[#] Ken-ichi Kato,[▽] and Yoshihiro Iwasa*[,†,‡]

Contribution from the Institute for Materials Research, Tohoku University, Katahira, Sendai 980-8577, Japan, CREST, Japan Science and Technology Corporation, Kawaguchi 330-0012, Japan, Japan Advanced Institute of Science and Technology, Tatsunokuchi, Ishikawa 923-1292, Japan, Department of Chemistry, University of Cambridge, Lensfield Road, Cambridge CB2 1EW, U.K., Department of Chemistry, Physics, and Environmental Science, University of Sussex, Brighton BN1 9QJ, U.K., Institute for Molecular Science, Myodaiji, Okazaki 444-8585, Japan, European Synchrotron Radiation Facility, BP 220, F-38043 Grenoble, France, and SPring-8, Japan Synchrotron Radiation Research Institute (JASRI), Hyogo 679-5198, Japan

Received October 9, 2002; E-mail: iwasa@imr.edu; K.Prassides@susx.ac.uk

Abstract: Intercalation of C_{70} with europium affords two kinds of magnetic compounds, a canted antiferromagnet Eu_xC_{70} ($x \approx 3$) and a ferromagnet Eu_xC_{70} ($x \approx 9$) with transition temperatures (T_C) of 5 and 38 K, respectively. The Curie constants in the paramagnetic phase and the saturation moment in the ferromagnetic phase are both understood by the full moment of Eu^{2+} for both systems. The structure of $Eu_{3-\delta}C_{70}$ ($\delta \approx 0.27$) is pseudo-monoclinic, derived by a simple deformation of the parent face-centered cubic (fcc) structure. $Eu_{9-\delta}C_{70}$ ($\delta \approx 0.2$) forms an fcc structure, in which cuboctahedral clustering of Eu^{2+} ions is observed in the enhanced size octahedral holes. The observed T_C of the $Eu_{9-\delta}C_{70}$ ferromagnet is comparable to or larger than those of simple binary Eu-based ferromagnets, such as Eu chalcogenides or carbides, despite the low atomic ratio of Eu in the chemical formulas. This can be understood by the short $Eu^{2+}-Eu^{2+}$ distances and high coordination numbers permitted by the multiple occupation by Eu^{2+} ions of the expanded octahedral interstitial sites in higher fullerene-based solids.

Introduction

Various novel aspects of fullerene-based magnets have recently attracted considerable interest. The discovery of weak ferromagnetism in rhombohedral C_{60} polymers at a remarkably high Curie temperature, $T_C \approx 500$ K, has demonstrated possible new routes to carbon-based magnets.[1] (TDAE)C_{60} (TDAE = tetrakis(dimethylamino)ethylene) has been a fascinating material, which exhibits the highest T_C (= 16 K) among molecular ferromagnets without magnetic elements.[2] While its structure, including the molecular orientations of the C_{60} units, has been determined in detail, conclusive understanding of the mechanism of the ferromagnetic interactions has not been reached as yet.[3] Fullerene-based solids with antiferromagnetic ground states have also been synthesized.[4] Structural analysis of the $(NH_3)K_3C_{60}$ antiferromagnet has revealed that the sign of magnetic interactions between C_{60}^{3-} anions depends on the relative orientations of neighboring molecules.[5] In all these systems, the unpaired spins reside on the C_{60} units. A different kind of fullerene-based molecular magnetic material was recently obtained by intercalation of C_{60} with europium metal. Following the exploration of the $Eu-C_{60}$ phase diagram,[6] Ishii *et al*. found Eu_6C_{60} to display ferromagnetic ordering of Eu^{2+} spins near 14 K which was accompanied by giant negative magnetoresistance.[7] Its magnetic structure was determined by powder neutron diffraction, and its configurational symmetry was determined as body-centered cubic (bcc) with a magnetic moment per Eu^{2+} ion of 7.1(3) μ_B.[8] This was the first observation of the magnetic order of the

[†] Tohoku University.
[‡] Japan Science and Technology Corporation.
[§] Japan Advanced Institute of Science and Technology.
[∥] University of Cambridge.
[⊥] University of Sussex.
[○] Institute for Molecular Science
[#] European Synchrotron Radiation Facility.
[▽] Japan Synchrotron Radiation Research Institute (JASRI).

(1) Makarova, T. L.; Sundqvist, B.; Hohne, R.; Esquinazi, P.; Kopelevich, Y.; Scharff, P.; Davydov, V. A.; Kashevarova, L. S.; Rakhmanina, A. V. *Nature* **2001**, *413*, 716.
(2) Allemand, P. M.; Khemani, K. C.; Koch, A.; Wudl, F.; Holczer, K.; Donovan, S.; Gruner, G.; Thompson, J. D. *Science* **1991**, *253*, 301.
(3) Narymbetov, B.; Omerzu, A.; Kabanov, V. V.; Tokumoto, M.; Kobayashi, H.; Mihailovic, D. *Nature* **2000**, *407*, 883.
(4) Takenobu, T.; Muro, T.; Iwasa, Y.; Mitani, T. *Phys. Rev. Lett.* **2000**, *85*, 381.
(5) Margadonna, S.; Prassides, K.; Shimoda, H.; Takenobu, T.; Iwasa, Y. *Phys. Rev. B* **2001**, *64*, 132414.
(6) Ksari-Habiles, Y.; Claves, D.; Chouteau, G.; Touzain, P.; Jeandey, C.; Oddou, J. L.; Stepanov, A. *J. Phys. Chem. Solids* **1997**, *58*, 1771. Claves, D.; Ksari-Habiles, Y.; Chouteau, G.; Touzain, P. *Solid State Commun.* **1998**, *106*, 431.
(7) Ishii, K.; Fujiwara, A.; Suematsu, H.; Kubozono, Y. *Phys. Rev. B* **2002**, *65*, 134431.
(8) Margiolaki, I.; Margadonna, S.; Prassides, K.; Hansen, T.; Ishii, K.; Suematsu, H. *J. Am. Chem. Soc.* **2002**, *124*, 11288.

10.1021/ja0288690 CCC: $25.00

spins of metal dopants in C_{60} solids. In addition, the ferromagnetic order of Eu^{2+} is in sharp contrast with the case of Eu intercalated graphite, EuC_6 which orders antiferromagnetically at 38 K.[9]

Motivated by the discovery of ferromagnetic order in Eu-intercalated C_{60} solids, we searched for new ferromagnetic materials based on C_{70}. In this paper, we report the synthesis, structural characterization, and observation of ferromagnetic order in the Eu-intercalated C_{70} compounds $Eu_{3-\delta}C_{70}$ and $Eu_{9-\delta}C_{70}$. $Eu_{3-\delta}C_{70}$ displays an antiferromagnetic interaction at high temperature and shows a magnetic transition below 5 K accompanied by the appearance of a small spontaneous moment. It is isostructural with $Sm_{2.78}C_{70}$, adopting a pseudo-monoclinic structure derived by deformation of the well-known fcc A_3C_{60} fulleride structures.[10] In $Sm_{2.78}C_{70}$, there are C_{70} dimers bridged by Sm ions.[11] $Eu_{9-\delta}C_{70}$ demonstrates the influence of the increased size of the interstitial holes in higher fullerenes, compared with C_{60}, in achieving higher metal doping levels. While in the case of C_{60}, bcc Eu_6C_{60} and K_6C_{60} are the saturation phases,[7,12] Eu and K doping of C_{70} yields Eu_9C_{70} and K_9C_{70}. The crystal structure of K_9C_{70} is fcc with multiple occupation by K of the octahedral sites.[13] Similar multiple occupation in the octahedral holes has been also encountered in K-doped C_{84} compounds[14] and Na and Li-doped C_{60}.[15] In C_{60}-based compounds, multiple occupation is only encountered for cations with ionic radii less than 1 Å, while that of larger cations is unfavorable. The structural model of $Eu_{9-\delta}C_{70}$ derived by Rietveld analysis shows that multiple occupation of the octahedral site indeed occurs and that Eu ions are disordered over the corners of a cuboctahedron. Magnetic measurements revealed that $Eu_{9-\delta}C_{70}$ is a ferromagnet with a surprisingly high T_C of 38 K. This is even higher than that of EuC_2,[16] in which the Eu concentration is much larger. We postulate that the formation of the cuboctahedral Eu cluster in Eu_9C_{70} is crucial in leading to enhanced magnetic interactions.

Experimental Section

The europium intercalated C_{70} samples were prepared from chromatographically purified and vacuum outgassed C_{70}. The diffraction patterns of thus obtained C_{70} powder revealed that it was a mixture of hexagonal and cubic phases with the hexagonal phase dominating. The structure of the intercalated phases did not depend on the starting ratio of hexagonal to cubic phase. High-purity europium metal was broken into powder and mixed with C_{70} in an atmosphere-controlled glovebox. Powder mixtures were pressed to pellets and loaded into quartz tubes, which were then sealed under a vacuum of 10^{-6} Torr. Heat treatments were carried out at temperatures of 400−650 °C for periods ranging from days to months. Overheating at temperatures higher than 500 °C led to the formation of europium carbide, EuC_2. Highly uniform samples with small carbide content were prepared by annealing for a month at 450 °C. The samples were then sealed in 0.5-mm and 2.0-mm diameter capillaries for X-ray and magnetometry experiments, respectively. Powder samples of about 10 mg were used for the magnetization measurements with a superconducting quantum interference device (SQUID) magnetometer. Synchrotron X-ray diffraction patterns of Eu_3C_{70} were recorded on an imaging plate installed on the BL02B2 beamline at the Super Photon Ring (SPring-8, Hyogo, Japan) at room temperature ($\lambda = 0.8507(1)$ Å). Data on Eu_9C_{70} were collected in continuous scanning mode using nine Ge(111) analyzer crystals on the BM16 beamline at the European Synchrotron Radiation Facility (ESRF, Grenoble, France) at 10 K ($\lambda = 0.82654$ Å) and were rebinned in the 2θ range 4°−28.5° to a step of 0.01°. Analysis of the diffraction data was performed with the Fullprof[17] and PROFIL[18] suites of Rietveld analysis programs, incorporating symmetry-adapted spherical-harmonic (SASH) functions for the description of spherically disordered molecules. X-ray absorption near edge structure (XANES) spectra were measured on the BL01B1 beamline at SPring-8 by the fluorescence method.

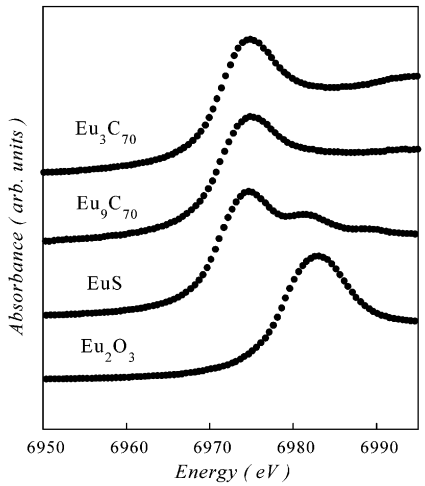

Figure 1. Eu L_{III}-edge XANES spectra of $Eu_{3-\delta}C_{70}$, $Eu_{9-\delta}C_{70}$, EuS, and Eu_2O_3.

Results

XANES Spectroscopy. The valence of Eu ions in the Eu_xC_{70} samples with nominal Eu contents of 3 and 9 was determined by Eu L_{III}-edge X-ray absorption near edge structure (XANES) experiments, as shown in Figure 1. The spectra of EuS and Eu_2O_3 were also measured as references of divalent and trivalent Eu compounds. The adsorption edges of both Eu_xC_{70} ($x \approx 3$, 9) compositions are very close to those of EuS, indicating that the Eu ion is divalent in C_{70} fullerides. Eu has also been found to be divalent in both intercalated graphite[9] and C_{60} fullerides.[7,8]

Structural Analyses. The Eu_xC_{70} phase diagram was first surveyed as a function of Eu nominal content, with x between 1 and 12. Powder X-ray diffraction measurements revealed that single-phase compositions are only encountered around doping levels, $x = 3$ and 9. The diffraction patterns for samples with x between 0 and 3 correspond to phase mixtures of undoped C_{70} and Eu_3C_{70}, precluding the existence of stable Eu_xC_{70} phases in this range. In contrast, the profiles obtained for nominal

(9) Suematsu, H.; Ohmatsu, K.; Yoshizaki, R. *Solid State Commun.* **1981**, *38*, 1103.
(10) Chen, X. H.; Chi, D. H.; Sun, Z.; Takenobu, T.; Liu, Z. S.; Iwasa, Y. *J. Am. Chem. Soc.* **2000**, *122*, 5729.
(11) Chi, D. H.; Iwasa, Y.; Chen, X. H.; Takenobu, T.; Ito, T.; Mitani, T.; Nishibori, E.; Takata, M.; Sakata, M.; Kubozono, Y. *Chem. Phys. Lett.* **2002**, *359*, 177.
(12) Zhou, O.; Fischer, J. E.; Coustel, N.; Kycia, S.; Zhu, Q.; McGhie, A. R.; Romanow, W. J.; J. P. M., Jr.; A. B. S., III; Cox, D. E. *Nature* **1991**, *351*, 462.
(13) Kobayashi, M.; Akahama, Y.; Kawamura, H.; Shinohara, H.; Sato, H.; Saito, Y. *Phys. Rev. B* **1993**, *48*, 16877.
(14) Allen, K. M.; Dennis, T. J. S.; Rosseinsky, M. J.; Shinohara, H. *J. Am. Chem. Soc.* **1998**, *120*, 6681.
(15) Rosseinsky, M. J.; Murphy, D. W.; Fleming, R. M.; Tycko, R.; Ramirez, A. P.; Siegrist, T.; Dabbagh, G.; Barrett, S. E. *Nature* **1992**, *356*, 416. Yildirim, T.; Zhou, O.; Fischer, J. E.; Bykovetz, N.; Strongin, R. A.; Cichy, M. A.; Smith, A. B.; Lin, C. L.; Jelinek, R. *Nature* **1992**, *360*, 569. Margadonna, S.; Prassides, K.; Fitch, A. N.; Kosaka, M.; Tanigaki, K. *J. Am. Chem. Soc.* **1999**, *121*, 6318.
(16) Sakai, T.; Adachi, G.; Yoshida, T.; Ueno, S.; Shiokawa, J. *Bull. Chem. Soc. Jpn.* **1982**, *55*, 699.
(17) Rodriguez-Carvajal, J. *Fullprof*, version 3.5; Illinois, 1997 (unpublished).
(18) Cockcroft, J. K. *PROFIL*; Birkbeck College: London, 1994.

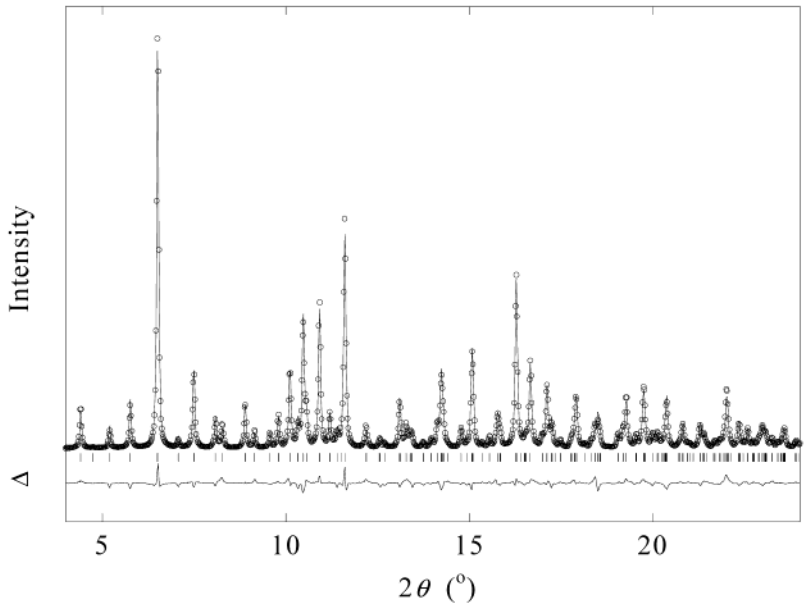

Figure 2. Final observed (○) and calculated (solid line) synchrotron X-ray ($\lambda = 0.8507$ Å) powder diffraction profile for $Eu_{2.73}C_{70}$ at room temperature. The lower solid line shows the difference profile, and the tick marks show the reflection positions.

contents between 3 and 9 are very complicated and do not correspond to mixtures of the Eu_3C_{70} and Eu_9C_{70} phases, implying the existence of additional intermediate phases, which could not be isolated under the present preparative conditions.

(a) $Eu_{3-\delta}C_{70}$. Figure 2 shows the synchrotron X-ray diffraction pattern of the Eu_xC_{70} ($x \approx 3$) phase at room temperature. There is a remarkable similarity of the recorded profile with that of $Sm_{2.78}C_{70}$ which crystallizes in a pseudo-monoclinic structure (space group $P1$, $a = 14.86(1)$ Å, $b = 10.09(1)$ Å, $c = 10.92(1)$ Å, $\alpha = 90°$, $\beta = 96.17(2)°$, $\gamma = 90°$).[10,11] A LeBail refinement of the $Eu_{3-\delta}C_{70}$ diffraction data was first employed to extract accurate values of the lattice parameters ($a = 14.932(2)$ Å, $b = 10.130(2)$ Å, $c = 10.960(1)$ Å, $\beta = 96.078(5)°$) by employing an analogous model to that of $Sm_{2.78}C_{70}$. We note that the a lattice parameter is comparable to that of the fcc structure of pristine C_{70} (14.93 Å), while the b and c lattice parameters straddle the magnitude of the shortest inter-C_{70} separations in the basal plane (10.56 Å) of the fcc unit cell. Thus, the unit cell of $Eu_{3-\delta}C_{70}$ can be regarded as deriving by a deformation of the fcc structure of C_{70} with Eu residing in the tetrahedral and octahedral interstices.

Rietveld analysis of the diffraction profile of $Eu_{3-\delta}C_{70}$ to the electron density level in analogy with $Sm_{2.78}C_{70}$ (ref 11) has proven difficult to perform because of the inferior quality of the present data. Instead, as the diffraction pattern of $Eu_{3-\delta}C_{70}$ is dominated by the contribution of the heavy Eu ions, we focused our attention in determining principally their position in the unit cell and their site occupation. As a result, even though the low crystal symmetry implies orientational ordering of the C_{70} ions, we approximated the fullerene molecules in the course of the refinement by employing a spherical shell model. This approach has been used before to describe the orientational disorder of fullerene units in their high temperature fcc phases.[19,20] Within this model, the carbon motion is confined to the surface of a sphere with the electronic density surface of each fullerene molecule described by a uniform spherical shell with the radius, R, and the molecular form factor, $f(\mathbf{Q})$, given by the zeroth-order Bessel function:

$$f(\mathbf{Q}) = [N/\sqrt{(4\pi)}]\, f_C[\sin(QR)/QR] \qquad (1)$$

where N is the number of C atoms, Q is the momentum transfer, and f_C, the carbon form factor. In an attempt to mimic an ellipsoidal shape, C_{70} was modeled in terms of two spherical shells with different dimensions. The starting values of the radii, $R_1 \approx 3.56$ Å and $R_2 \approx 3.98$ Å, were obtained from the lengths of the C_{70} short and long axes. The total carbon scattering density was equally distributed between the two shells. The starting positions of the Eu ions were identical to those of Sm in $Sm_{2.78}C_{70}$.[11] The results of the fit are summarized in Table 1 and shown as a solid line in Figure 2, while the structural model of $Eu_{3-\delta}C_{70}$ is schematically displayed in Figure 3. The coordinates and occupancies of the Eu ions refine to values very close to those of $Sm_{2.78}C_{70}$. The low crystal symmetry necessitates the presence of two symmetry-inequivalent pseudo-octahedral Eu positions at (x,y,z) with $x \approx 0$, $y \approx 1/2$, $z \approx 1/2$

Table 1. Final Results of the Rietveld Refinement of the Synchrotron X-ray Powder Diffraction Profile of $Eu_{3-\delta}C_{70}$ at Room Temperature (Space Group $P1$, $\chi^2 = 6.6\%$, $R_{exp} = 2.4\%$)[a]

	x/*a*	*y*/*b*	*z*/*c*	U_{iso}/Å^2	occupancy
C_{70}(I)	0	0	0	0.042(2)	1
C_{70}(II)	1/2	1/2	1/2	0.042(2)	1
Eu(1)	0.22(1)	0.00(1)	0.51(1)	0.021(2)	1.000(3)
Eu(2)	0.76(1)	0.00(1)	0.47(1)	0.021(2)	0.992(5)
Eu(3)	0.26(1)	0.47(1)	0.04(1)	0.021(2)	0.474(6)
Eu(4)	0.73(1)	0.50(1)	0.02(1)	0.021(2)	0.996(5)
Eu(5)	0.97(1)	0.51(1)	0.63(1)	0.021(2)	0.500(3)
Eu(6)	0.10(1)	0.53(1)	0.71(1)	0.021(2)	0.500(3)
Eu(7)	0.40(1)	0.14(1)	0.02(1)	0.021(2)	0.500(3)
Eu(8)	0.43(1)	0.91(1)	0.01(1)	0.021(2)	0.500(3)

[a] The refined cell constants and the final composition were $a = 14.926(2)$ Å, $b = 10.130(1)$ Å, $c = 10.950(1)$ Å, $\beta = 96.111(5)°$, and $Eu_{2.73(3)}C_{70}$, respectively. The inner and outer shell radii of the C_{70} units were $R_1 = 3.68(5)$ Å and $R_2 = 4.02(7)$ Å, respectively.

(19) Heiney, P. A.; Fischer, J. E.; McGhie, A. R.; Romanow, W. J.; Denenstein, A. M.; McCauley, J. P., Jr.; Smith, A. B. *Phys. Rev. Lett.* **1991**, *66*, 2911.
(20) Margadonna, S. M.; Brown, C. M.; Dennis, T. J. S.; Lappas, A.; Pattison, P.; Prassides, K.; Shinohara, H. *Chem. Mater*. **1998**, *10*, 1742.

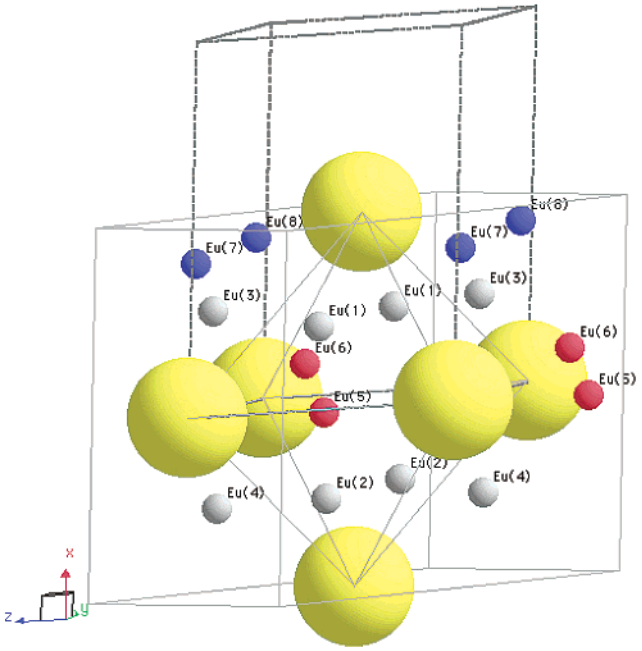

Figure 3. Schematic representation of the crystal structure of $Eu_{2.73}C_{70}$. The quasi-monoclinic and the parent fcc unit cells are represented by dotted and solid lines, respectively. Large yellow spheres represent C_{70} molecules. Small gray spheres are tetrahedral Eu^{2+} ions, and blue and red spheres, off-centered octahedral Eu^{2+} ions.

(Eu(5)) and $x \approx {}^1/_2$, $y \approx 0$, $z \approx 0$ (Eu(7)) and four symmetry-inequivalent pseudo-tetrahedral Eu positions (Eu(1−4)). In analogy with $Sm_{2.78}C_{70}$, we find that each Eu residing in the large octahedral interstices is disordered over two sites each with an occupancy of $\sim{}^1/_2$. No such positional disorder is encountered for Eu(1−4) in the smaller tetrahedral holes. However, when their occupation numbers were allowed to vary, a stable refinement was obtained with the Eu(1), Eu(2), and Eu(4) sites essentially fully occupied, while the occupancy of the Eu(3) site converged to $\sim{}^1/_2$ (Table 1), leading to a refined stoichiometry of $Eu_{2.73(3)}C_{70}$. The presence of tetrahedral vacancies is reminiscent of other rare earth fullerides ($Sm_{2.78}C_{70}$, $Yb_{2.75}C_{60}$)[11,21] and appears to be a characteristic feature of lanthanide fullerides with a metal doping level close to 3. The absence of superlattice reflections, which are present in the $Yb_{2.75}C_{60}$ diffraction profile,[21] suggests that the tetrahedral vacancies in $Eu_{2.73}C_{70}$ are distributed randomly. The presence of the vacancies is also reflected in the positional parameters of the pseudo-octahedral Eu ions which shift away from the site center toward the partially occupied Eu(3) sites. One puzzling feature which remains to be understood is that the unit cell of $Eu_{2.73}C_{70}$ is somewhat larger (by ∼1%) than that of its Sm counterpart, even though the ionic radius of Eu^{2+} is smaller than that of Sm^{2+}. This might perhaps indicate the presence of an Sm^{2+}/Sm^{3+} mixed valence in $Sm_{2.78}C_{70}$.

(b) $Eu_{9-\delta}C_{70}$. Figure 4 displays the synchrotron X-ray diffraction pattern for the sample with nominal composition, $Eu_{9-\delta}C_{70}$. The observed reflections are extremely broad compared with those of $Eu_{2.73}C_{70}$, indicative of a much inferior crystallinity. No changes in the measured diffraction profile were observed for nominal x values larger than 9, implying that it corresponds to a saturation phase. Most of the peaks observed to a momentum transfer $Q = 3.42$ Å^{-1} (where $Q = 4\pi \sin\theta/\lambda$) were indexed with Miller indices either all odd or all even, consistent with a fcc structure for $Eu_{9-\delta}C_{70}$. The few exceptions ($2\theta = 13°$, 16.1°, 18.5°, and 26.3°) were ascribed to the presence of small amounts of impurities. Attempts to index the extra peaks showed the absence of unreacted Eu metal, EuC_2, hexagonal close packed (hcp), or rhombohedral C_{70} phases in the sample. Rietveld refinements of the profile were thus attempted in space group $Fm\bar{3}m$. This necessitates the presence of orientationally disordered quasi-spherical fullerene units. Despite the lower symmetry (D_{5h}) compared with that of C_{60} (I_h) and its ellipsoidal shape, C_{70} could be still modeled as quasi-spherical (vide supra) as the molecular anisotropy is averaged out by static and/or dynamic orientational disorder. Deviations from perfect sphericity, described by eq 1, can be studied by assuming that, for atoms confined to a spherical shell, the orientational scattering density function can be defined in terms of symmetry-adapted spherical-harmonic (SASH) functions.[22] The molecular form factor, $f(\mathbf{Q})$ can be expressed as

$$f(\mathbf{Q}) = \sqrt{(4\pi)}\, f_C \sum_l \sum_\nu i^l j^l(QR) C_{l\nu} K_{l\nu}(\theta_Q,\phi_Q) \qquad (2)$$

where $j^l(QR)$ are the l-th order spherical Bessel functions, $K_{l\nu}(\theta,\phi)$ are the SASH functions, obtained from linear combinations of spherical harmonic functions, $Y_{lm}(\theta,\phi)$, and $C_{l\nu}$ are refinable coefficients. The first term in the expansion corresponds to the ideal spherical shell, while the higher order SASH terms modulate the deviations from ideality. Only the coefficients transforming as the totally symmetric representation of the point group of the site symmetry of the shell of atoms are nonzero, and they can be evaluated in the course of the Rietveld refinement. The integer ν labels the particular representation within A_{1g} for a given value of l.

As mentioned before, Rietveld refinements of the $Eu_{9-\delta}C_{70}$ diffraction profile were initiated in the space group $Fm\bar{3}m$. The ellipsoidal shape of C_{70} was again modeled in terms of two spherical shells with radii $R_1 \approx 3.56$ Å and $R_2 \approx 3.98$ Å. The total carbon scattering density was equally distributed between the two shells, and the pronounced orientational disorder was modeled in terms of SASH functions in both of them. The two shells were placed at the 4*a* sites of $m\bar{3}m$ (O_h) symmetry in the fcc lattice. This positioning only necessitates consideration of the SASH functions, $K_{l\nu}(\theta,\phi)$, with values for $l = 0$, 4, 6, 8, and 10.

The retention of fcc packing in the europium-saturated phase suggests that Eu cations occupy the tetrahedral (T) site, while the larger octahedral (O) interstitial site is multiply occupied. In analogy with the fcc phases of $Na_{6+x}C_{60}$, Li_3CsC_{60}, K_9C_{70}, and $K_{8+x}C_{84}$,[13−15] Rietveld refinements were initiated with the Eu cations placed in the center of the O and T sites, with the excess Eu in (x,x,x) positions ($x \approx 0.64$) which describe a cube produced by displacement away from the center of the octahedral site parallel to the [111] directions. Within this model, the

(21) Ozdas, E.; Kortan, A. R.; Kopylov, N.; Ramirez, A. P.; Siegrist, T.; Rabe, K. M.; Bair, H. E.; Schuppler, S.; Citrin, P. H. *Nature* **1995**, *375*, 126.

(22) Press, W.; Hüller, A. *Acta Crystallogr. A* **1973**, *29*, 252. Michel, K. H.; Copley, J. R. D.; Neumann, D. A. *Phys. Rev. Lett.* **1992**, *68*, 2929. Chow, P. C.; Jiang, X.; Reiter, G.; Wochner, P.; Moss, S. C.; Axe, J. D.; Hanson, J. C.; McMullan, R. K.; Meng, R. L.; Chu, C. W. *Phys. Rev. Lett.* **1992**, *69*, 2943. Hirosawa, I.; Prassides, K.; Mizuki, J.; Tanigaki, K.; Gevaert, M.; Lappas, A.; Cockcroft, J. K. *Science* **1994**, *264*, 1294. Margadonna, S.; Prassides, K.; Fitch, A. N.; Kosaka, M.; Tanigaki, K. *J. Am. Chem. Soc.* **1999**, *121*, 6318.

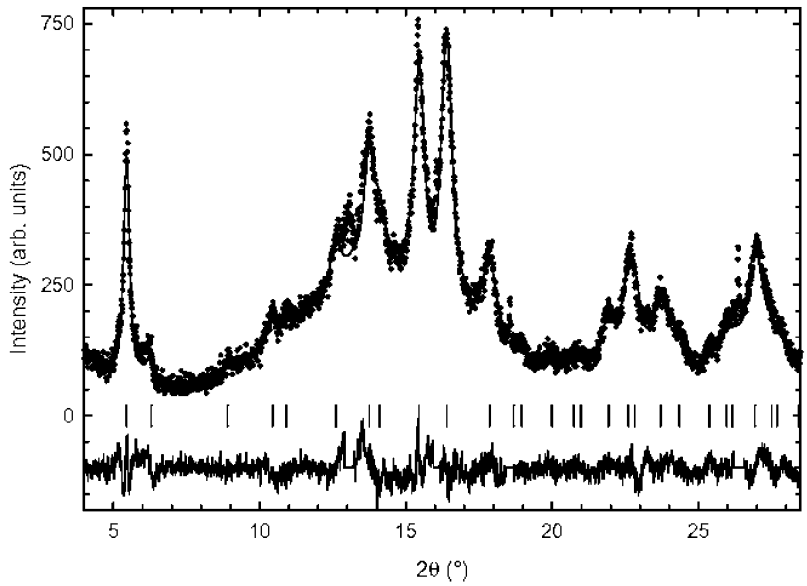

Figure 4. Final observed (○) and calculated (solid line) synchrotron X-ray ($\lambda = 0.82654$ Å) powder diffraction profile for $Eu_{8.8}C_{70}$ at 10 K. The lower solid line shows the difference profile, and the tick marks show the reflection positions.

results were unsatisfactory, leading to negative thermal parameters for the C_{70} spherical shells and the Eu atoms. In addition, the intensities were not reproduced adequately ($\chi^2 > 5.0$), indicating a different arrangement of the Eu cations within the large octahedral sites. As the scattering form factor of Eu is extremely large, a detailed exploration of difference Fourier maps was undertaken. This readily revealed an extra electron density located on the (110) plane at the position (0.6,0.1,0), which, in the $Fm\bar{3}m$ space group, is the 48*i* special position and describes a cuboctahedron around the center of the octahedral hole. The model structure is shown in Figure 5. The quality of the Rietveld refinements with the excess Eu cations located in (0.6,0.1,0) improved significantly leading to a final agreement factor, $\chi^2 = 2.1$ (lattice constant $a = 15.0572(16)$ Å). The refined values of the radii of the two spherical shells ($R_1 = 3.71(9)$ Å and $R_2 = 4.06(7)$ Å) were physically meaningful, while the refined composition converged to $Eu_{8.8(2)}C_{70}$, in good agreement with the starting nominal stoichiometry. The individual fractional occupancies indicated 72(2)% occupation of the tetrahedral site, 58(1)% occupation of the center of the octahedral site, and 56(1)% occupation of the cuboctahedral defect positions. The final results of the Rietveld refinement are summarized in Table 2, and the Eu−Eu distances are given in Table 3.

The poor crystallinity of the $Eu_{8.8}C_{70}$ sample and the lack of scattered intensity in the diffraction profile at high *Q* necessitate that the refined structural model should be considered with care. Ideally, alternative models of the orientational disorder of the C_{70} units, based on discrete molecular orientations, should have been explored. The quality of the data precludes such exploration, but we note that the two-shell model with higher-order SASH coefficients consistently led to improved quality refinements compared with those of single shell models, precisely implying the existence of such locally ordered molecular orientations, which are partially modeled. Deficiencies in the correct description of the C_{70} orientations could also affect the cation positions and their occupancies, especially for such a heavily disordered material. However, given the heavily scattering power of the Eu ions, we found the Fourier map explorations were always conclusively demonstrating that the Eu ions reside in the regular octahedral and tetrahedral sites as well as in the defect cuboctahedral site. Displacement of the latter to a number of other candidate defect sites always led to severe degradation of the quality of the fit. Still, its temperature factor, U_{iso}, was refined to a large value of 0.48 Å^2, indicative of possible correlations with its position and occupation factor. We note, however, that site displacement parameters as large as 0.4 Å^2 have been reported before in A_3C_{60} and A_3C_{70}

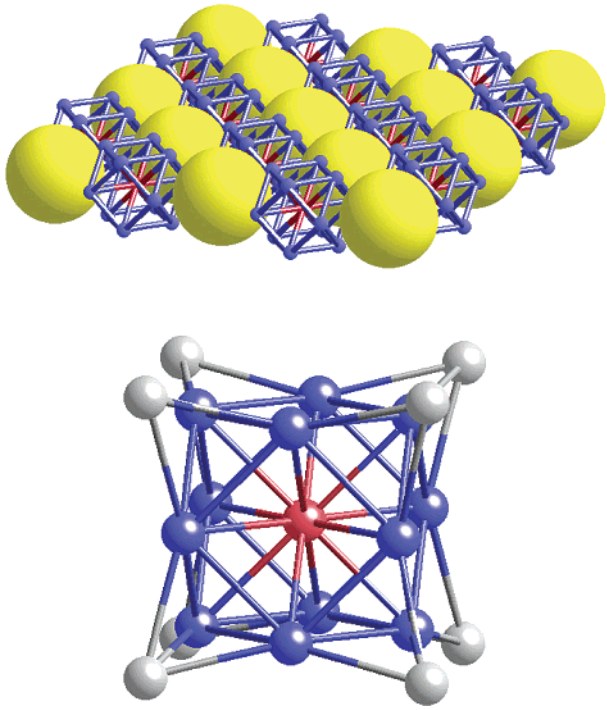

Figure 5. (Top) Schematic diagram of the (001) plane in the fcc $Eu_{8.8}C_{70}$ crystal structure. The C_{70} units are represented as yellow spheres, and the Eu(2) and Eu(3) ions, as small blue and red spheres, respectively. (Bottom) The Eu_{12} cuboctahedron residing in the octahedral interstices. Blue, gray, and red spheres represent defect Eu(2), tetrahedral Eu(1), and octahedral Eu(3) ions, respectively.

Table 2. Final Results of the Rietveld Refinement of the Powder X-ray Diffraction Profile of $Eu_{9-\delta}C_{70}$ at 10 K (Space Group $Fm\bar{3}m$, $\chi^2 = 2.1$, $R_{exp} = 11.1\%$)[a]

	x/a	y/b	z/c	U_{iso}/Å^2	occupancy
C_{70}	0	0	0		1
Eu(1)	$^1/_4$	$^1/_4$	$^1/_4$	0.02	0.72(2)
Eu(2)	0.6917(4)	0.1917(4)	0	0.48	0.56(1)
Eu(3)	$^1/_2$	$^1/_2$	$^1/_2$	0.008	0.58(1)

[a] The refined cell constant and the final composition were a = 15.0572(16) Å and $Eu_{8.8(2)}C_{70}$, respectively. Other data are as follows: inner shell radius, 3.71(9) Å; cubic harmonic coefficients, $C_{0,1} = 1$, $C_{4,1} = -6.9(3)$, $C_{6,1} = 0.6(2)$, $C_{8,1} = -7.1(6)$, $C_{10,1} = 1.3(3)$; $U_{iso} = 0.04(1)$ Å^2; outer shell radius, 4.06(7) Å; cubic harmonic coefficients, $C_{0,1} = 1$, $C_{4,1} = 7.8(2)$, $C_{6,1} = 2.3(2)$, $C_{8,1} = 7.9(5)$, $C_{10,1} = -9.5(6)$; $U_{iso} = 0.11(1)$ Å^2.

Table 3. Eu−Eu Distances (Å) in $Eu_{9-\delta}C_{70}$ at 10 K

edge of Eu_{12} cuboctahedron	4.085(7)
octahedral site to corner	4.085(7)
tetrahedral site to corner	3.964(2)
between cuboctahedra	2.477(9)

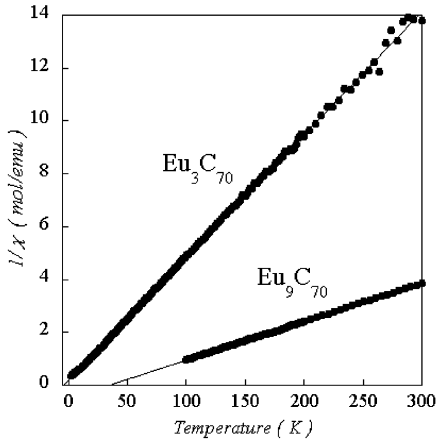

Figure 6. Temperature dependence of the reciprocal molar susceptibility, $1/\chi$, of $Eu_{3-\delta}C_{70}$ and $Eu_{9-\delta}C_{70}$. The filled circles are the experimental data, and the lines are fits to the Curie−Weiss law.

structures.[23,24] Such large displacements are the signatures of static and/or thermal disorder.

Magnetic Properties. Figure 6 displays the temperature dependence of the reciprocal molar susceptibility, $1/\chi$, for Eu_xC_{70} ($x \approx 3$, 9). At high temperatures, χ is well described by the simple Curie−Weiss expression, $\chi = C/(T-\Theta)$, for both systems, where C is the Curie constant and Θ is the Weiss temperature. The effective magnetic moments per europium atom, μ_{eff}, were derived as 7.71(1) μ_B and 7.82(1) μ_B for x = 3 and 9, respectively. These values agree well with the expected moment for Eu^{2+} ions with ^8S configuration ($J = ^7/_2$, $L = 0$, $gJ = 7$; $\mu_{eff} = 7.937\ \mu_B$). The Weiss temperatures, Θ, are −4.2(1) K and 33.9(2) K for $x = 3$ and 9, respectively. A small but negative Weiss temperature in $Eu_{3-\delta}C_{70}$ indicates that magnetic interactions between Eu^{2+} ions are antiferromagnetic. The large positive Weiss temperature in $Eu_{9-\delta}C_{70}$, on the other hand, provides strong evidence for ferromagnetic interactions between Eu ions.

Figure 7 shows the magnetization curves at 2 K, 50 K (100 K), and 300 K for both compounds. Here, the magnetization, M, is converted to number of Bohr magnetons per Eu atom. The saturation moments at 2 K are close to 7 μ_B, again as expected for the +2 oxidation state of Eu for both compounds. However, there exists a considerable difference in the magnetization process at low fields. In contrast to the sharp rise in $Eu_{9-\delta}C_{70}$, the magnetization in $Eu_{3-\delta}C_{70}$ increases gradually. In combination with its negative Weiss temperature, which is consistent with the presence of antiferromagnetic interactions, the magnetic state of $Eu_{3-\delta}C_{70}$ can be understood as a canted antiferromagnet. $Eu_{9-\delta}C_{70}$, on the other hand, behaves as a typical ferromagnet, though we did not observe any hysteretic behavior in the magnetization curves at 2 K within the experimental uncertainty.

Figure 8 shows the measured magnetization, M, as function of temperature for the samples cooled at low applied fields (1 and 10 Oe). M increases sharply below T_C = 5 and 38 K for $Eu_{3-\delta}C_{70}$ and $Eu_{9-\delta}C_{70}$, respectively. These critical temperatures differ markedly from those of possible impurities, like EuC_2 (T_C = 20 K)[16] and EuO (T_C = 77 K).[25] Additional evidence supporting long-range ferromagnetic order in Eu_9C_{70} comes from measurements of the field dependence of the Curie temperature, T_C, shown in the inset of the right panel of Figure 8. Here, T_C is defined by the intersection of linear extrapolations of the $M(T)$ curves from above and below the rapid rise in $M(T)$ and increases approximately linearly up to 5 kOe, a typical behavior of ferromagnetic materials. In addition, the sharp rise of M below T_C was also observed in *ac* susceptibility measurements.

Discussion

While the intercalation chemistry of C_{60} has been developed extensively, only few examples of well-characterized intercalated C_{70} fullerides exist in the literature.[10,11,13,24] This is presumably related to the nonspherical symmetry of the C_{70} molecule, which has prohibited the facile synthesis of crystalline A_xC_{70} solids over a broad range of dopant levels, x. When C_{60} is compared, two features of the intercalation chemistry of C_{70} arising from its larger molecular size are noteworthy. First, lanthanide ions such as Sm^{2+} and Eu^{2+} can fit, without severe electrostatic constraints, in the tetrahedral holes of the fcc C_{70} structure which have expanded to ~1.2 Å. Both $Sm_{2.78}C_{70}$ and $Eu_{2.73}C_{70}$ are stable well-crystalline phases with pseudo-monoclinic crystal structures, necessitated by the low-symmetry orientationally ordered C_{70} units. Both are also characterized by a multiple cation occupancy of the expanded octahedral site (to ~2.2 Å) in contrast with $Yb_{2.75}C_{60}$, where the smaller octahedral site (~1.7 Å) is singly occupied. Second, the increased size of the tetrahedral interstitial sites leads to saturated phases of C_{70} formed by reaction with excess lanthanide metals to retain fcc symmetry ($Eu_{8.8}C_{70}$, $r(Eu^{2+}) = 1.12$ Å $< r_{tetr}$), in contrast with C_{60}, where body-centered cubic (bcc) phases (Eu_6C_{60}, $r(Eu^{2+}) > r_{tetr}$) are formed. In addition, an increased Eu^{2+}-to-fullerene doping ratio from 6 to 8.8(2) can be attained.

Figure 4 (bottom) shows the Eu_{12} cuboctahedral cluster occupying the octahedral interstitial site in $Eu_{8.8}C_{70}$ with the Eu−Eu distances summarized in Table 3. The Eu−Eu edge distances are 4.085(7) Å, larger than the Eu−Eu distance in europium metal of 3.967 Å and thus necessitating no unusual interaction between Eu^{2+} ions. Comparable physically meaning-

(23) Bendele, G. M.; Stephens, P. W.; Fischer, J. E. *Europhys. Lett.* **1998**, *41*, 553.
(24) Denning, M. S.; Watts, I. D.; Moussa, S. M.; Durand, P.; Rosseinsky, M. J.; Tanigaki, K. *J. Am. Chem. Soc.* **2002**, *124*, 5570.
(25) Matthias, B. T.; Bozorth, R. M.; van Vleck, J. H. *Phys. Rev. Lett.* **1961**, *7*, 160.

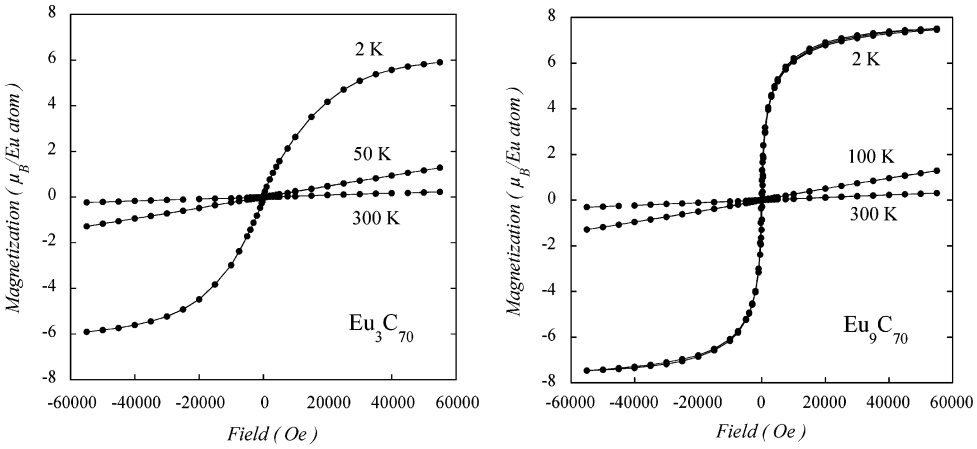

Figure 7. Magnetization in μ_B/Eu atom versus magnetic field, H, at temperatures of 2 K, 50 K (100 K), and 300 K for $Eu_{3-\delta}C_{70}$ (left) and $Eu_{9-\delta}C_{70}$ (right).

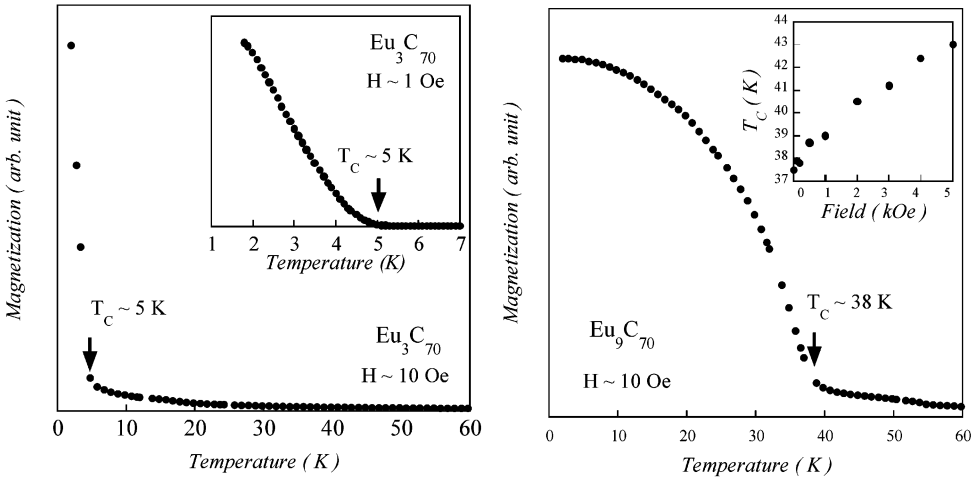

Figure 8. Magnetization versus temperature for $Eu_{3-\delta}C_{70}$ (left panel) and $Eu_{9-\delta}C_{70}$ (right panel) measured upon cooling in applied fields of ~10 Oe and ~1 Oe. The field dependence of T_C for $Eu_{9-\delta}C_{70}$ is shown in the inset.

ful values are also found for the distances from the octahedral and tetrahedral site centers to the cuboctahedron corners of 4.085(7) Å and 3.964(2) Å, respectively. On the other hand, as it is evident in Table 3, there are very short 2.5-Å contacts between the corners of neighboring Eu_{12} units. However, we recall that the refined Eu^{2+} site occupancies show that approximately only 50% of these corners are occupied. An attractive model is then to assume that the corners of adjacent cuboctahedra are occupied in a mutually exclusive way, thereby removing the presence in the structure of unphysically short contacts. This is also consistent with the apparent absence of any Eu solid solution behavior in $Eu_{8.8}C_{70}$ despite the large vacancy concentration, as increased occupancy of these positions is prohibited.

In $Eu_{2.73}C_{70}$, the Eu−Eu distances in the multiply occupied octahedral sites are very short (2.05(36) Å and 2.38(26) Å), but as the defect sites are only 50% occupied, their occupation is mutually exclusive. Distances, comparable to those in $Eu_{8.8}C_{70}$, are encountered between the partially occupied tetrahedral $Eu^{2+}(3)$ ion and the octahedral defects $Eu^{2+}(7)$ and $Eu^{2+}(6)$ (3.96(35) Å and 4.16(35) Å, respectively). However, in analogy with $Yb_{2.75}C_{60}$,[21] it is tempting to assume that simultaneous occupation of $Eu^{2+}(3)$ and $Eu^{2+}(7)$ or $Eu^{2+}(6)$ is also avoided, thereby leading to all Eu−Eu distances exceeding 5.61(37) Å. Finally, as there are insufficient data to refine the fullerene geometry, we employed eqs 1 and 2 to describe the form factor of C_{70}. The refined cubic harmonic coefficients of the two C_{70} shells in $Eu_{8.8}C_{70}$ (Table 2) indicate large deviations from perfect spherical symmetry, implying the existence of at least partial orientational order. This is also borne out by the fact that, for spherically disordered C_{70} units, nearest Eu−C distances of less than 2.82 Å (the sum of the ionic radius of Eu^{2+} and the van der Waals radius of C) are encountered. A similar situation is also found in $Eu_{2.73}C_{70}$.

In both intercalated fulleride solids $Eu_{3-\delta}C_{70}$ and $Eu_{9-\delta}C_{70}$, magnetic transitions are encountered at low temperature (5 and 38 K, respectively). For $Eu_{3-\delta}C_{70}$, the negative Weiss temperature, Θ (−4.2 K), and the gradual increase of the magnetization with applied magnetic field indicate a canted antiferromagnetic state. $Eu_{9-\delta}C_{70}$, on the other hand, behaves as a typical ferromagnet. The absences of hysteresis and coercive force in the magnetization curves are characteristic of soft ferromagnetic behavior. However, this may be related to the poor crystallinity of the samples, in analogy with the early results on the (TDAE)-C_{60} ferromagnet,[2] in which hysteresis was only observed subsequently in samples of improved quality.[26] The Curie temperatures, T_C, of the present Eu fullerides are comparable to or even larger than those of conventional simple Eu-based

(26) Suzuki, A.; Suzuki, T.; Whitehead, R. J.; Maruyama, Y. *Chem. Phys. Lett.* **1994**, *223*, 517.

Table 4. Nearest-Neighbor Shortest $Eu^{2+}-Eu^{2+}$ Distances (Å) and Curie Temperatures, T_C (K), in Binary Eu Solids and Eu-Intercalated Fullerides

EuO	3.64	77
EuC_2	4.12	20
EuS	4.21	16
Eu_6C_{60}	3.89	12
$Eu_{2.73}C_{70}$	5.6	5
$Eu_{8.8}C_{70}$	3.96, 4.09	38

ferromagnets, such as chalcogenides and carbides. In particular, a T_C of 38 K in $Eu_{9-\delta}C_{70}$ is unusually high when the Eu^{2+} concentration in this compound is compared with that in other binary Eu^{2+} ferromagnets.

The origin of the ferromagnetic exchange interactions between Eu^{2+} has been already investigated extensively in Eu_6C_{60}, which also shows conducting and giant magnetoresistive (GMR) behavior.[7] In addition, its T_C is affected little upon dilution of the Eu lattice by Sr substitution to form isostructural $Eu_{6-y}Sr_yC_{60}$ ($y = 3, 5$). The ferromagnetic transition is unchanged even in $EuSr_5C_{60}$, in which there is no three-dimensional Eu network, implying that the exchange interactions between the 4f electrons are indirect, modulated by the $\pi(C_{60})$ orbitals. This is also supported by the presence of short Eu−C contacts encountered in the structure[8] which are suggestive of hybridization between the 5d and 6s orbitals of Eu and the t_{1g} orbitals of C_{60}. Such a mechanism contrasts with the direct exchange ferromagnetic interaction of nearest neighbor 5d−4f unpaired electrons implicated in conventional binary Eu ferromagnets, like EuO, EuS, and EuC_2.[27] In these systems, T_C scales with the nearest $Eu^{2+}-Eu^{2+}$ distance (Table 4) and is unaffected by dilution of the Eu site by nonmagnetic ions.

Unlike Eu_6C_{60}, the Eu−C_{70} interactions could not be explicitly determined with the present data for $Eu_{3-\delta}C_{70}$ and $Eu_{9-\delta}C_{70}$ and information is thus only available for the Eu−Eu coordination environment. In $Eu_{2.73}C_{70}$, nearest Eu contacts of 4.0−4.2 Å are present but these are between partially occupied (50%) tetrahedral and octahedral sites, whose simultaneous occupation is probably prohibited in analogy with $Yb_{2.75}C_{60}$.[21] All other contacts are significantly longer (>5.6 Å), much larger than those encountered in both Eu_6C_{60} (3.89 Å) and the binary systems (∼3.64−4.21 Å) (Table 4). These structural features are in qualitative agreement with the magnetic properties of $Eu_{2.73}C_{70}$, which strongly indicate that it is a canted antiferromagnet with rather small antiferromagnetic interactions. On the other hand, T_C (38 K) in $Eu_{8.8}C_{70}$ is surprisingly high, even higher than that in europium carbide, EuC_2, which has a significantly larger Eu content. Despite its complicated structure, the origin of this effect in $Eu_{8.8}C_{70}$ could be traced to the enhanced size of the octahedral sites in C_{70} intercalated fullerides. In the saturated phases, this allows multiple occupation of the site and reduced metal contacts through the accommodation of large clusters, namely the cuboctahedral Eu_{12} cluster in the present system in which there is a multiplicity of short Eu−Eu contacts of 4.09 Å, comparable to the metal atom distances in Eu metal. Additional short distance exchange pathways also exist between the tetrahedral sites and the centers of the octahedral sites to the corners of the cuboctahedron (3.96 and 4.09 Å, respectively).

Conclusion

To summarize, we have synthesized two new Eu-doped C_{70} phases, Eu_xC_{70} ($x \approx 3, 9$) with magnetic transition temperatures, T_C, at 5 and 38 K, respectively. $Eu_{2.73}C_{70}$ adopts a pseudo-monoclinic structure, derived by a distortion of the parent fcc A_3C_{60} fulleride structure. The structure is identical to that of $Sm_{2.78}C_{70}$, in which Sm-bridged C_{70} dimer units are formed. The structure of $Eu_{8.8}C_{70}$ is fcc and accommodates a partially occupied cuboctahedral cluster of Eu ions in the expanded octahedral hole. $Eu_{2.73}C_{70}$ is a canted antiferromagnet with a small antiferromagnetic interaction in qualitative agreement with the large Eu−Eu distances encountered. $Eu_{8.8}C_{70}$, on the other hand, behaves as a typical ferromagnet. We also note that $T_C =$ 38 K in $Eu_{8.8}C_{70}$ is almost twice as high as that in EuC_2 ($T_C =$ 20 K), in which the Eu content per formula unit is 4−5 times higher than that in intercalated fullerides. The observed behavior might be attributed to the multiplicity of short Eu−Eu distances in $Eu_{8.8}C_{70}$, arising from the multiple occupation by the Eu^{2+} ions of the expanded octahedral interstitial sites. Intercalation of higher fullerene solids with rare earth elements thus provides an effective route to realize short interionic distances and high coordination numbers that help to stabilize the ferromagnetic states at high temperature. The present results indicate that the design of higher fullerene derivatives with a multiple occupation of interstitial holes could provide families of fullerene-based materials with novel electronic and magnetic functionalities.

Acknowledgment. We thank M. Sakata, M. Takata, and E. Nishibori for experimental help and the ESRF and Spring-8 for the provision of beamtime. We are grateful to Y. Taguchi for enlightening discussions. This work was partially supported by a Grant-in-Aid from the Japanese Ministry of Education, Culture, Sports, Science, and Technology.

JA0288690

(27) Kasuya, T. *IBM J. Res. Dev.* **1970**, *14*, 214.